

The massive elliptical galaxy NGC 4649 from the perspective of extended gravity

M. A. Jiménez, G. Garcia, X. Hernandez

Instituto de Astronomía, Universidad Nacional Autónoma de México, Apartado Postal 70-264 C.P. 04510 México D.F. México.

14 October 2018

ABSTRACT

Elliptical galaxies are systems where dark matter is usually less necessary to explain observed dynamics than in the case of spiral galaxies, however there are some instances where Newtonian gravity and the observable mass are insufficient to explain their observed structure and kinematics. Such is the case of NGC 4649, a massive elliptical galaxy in the Virgo cluster for which recent studies report a high fraction of dark matter, 0.78 at $4R_e$. However this galaxy has been studied within the MOND hypothesis, where a good agreement with the observed values of velocity dispersion is found. In a similar way, we have constructed a self-consistent gravitational equilibrium dynamical model for this galaxy assuming a modified gravity force law, which is equivalent to MOND for $a < a_0$ and recovers the Newtonian values for $a > a_0$. The modified gravity regime will be characterised by centrifugal equilibrium or dispersion velocities which become independent of distance, and which scale with the fourth root of the total baryonic mass, $V^4 \propto (MGa_0)$. We find that the recent detailed observations of the surface brightness profile and the velocity dispersion profile for this galaxy are consistent with the phenomenology expected in MONDian theories of modified gravity, without the need of invoking the presence of any hypothetical dark matter.

Key words: gravitation — stellar dynamics — NGC 4649 — stars: kinematics — elliptical galaxy: general

1 INTRODUCTION

The flat rotation curves of spiral galaxies have been well known for decades, e.g., Bosma (1981); Rubin et al. (1982), assuming the validity of the Newtonian law of gravity throughout, this results in a discrepancy between the dynamical mass and luminous mass of spiral galaxies. Other types of galaxies exhibit mass discrepancies as well, the most remarkable is the case of dwarf spheroidal galaxies for which the velocity dispersion is well known and the mass inferred from their internal dynamics greatly exceeds the mass visible by factors reaching into the thousands e.g., Simon & Geha (2007). On the other hand, bright giant elliptical galaxies exhibit small mass discrepancies e.g., Romanowsky et al. (2003), usually these facts are commonly interpreted as the manifestation of the dark matter halo in which the different galaxies are immersed. This halo dominates the dynamic of extended galaxies with low surface brightness, and its presence is less significant in more centrally concentrated galaxies with larger surface brightness values, e.g., McGaugh & de Blok (1998).

Alternatively, the discrepancy between observable mass in galaxies and their dynamics can be interpreted as a direct evidence for the failure of the current Newtonian and general

relativistic theories of gravity, rather than the existence of a dark matter component. As examples, in spiral galaxies the flat rotation curve has been successfully interpreted assuming a modification of Newtonian dynamics (MOND), e.g., Sanders & McGaugh (2002), or equivalently an extended Newtonian force law, e.g., Mendoza et al. (2011), the projected surface density profiles and observational parameters of the local dSph galaxies are in agreement with a description in MOND, e.g. Hernandez et al. (2010); McGaugh & Wolf (2010); Kroupa et al. (2010). Similarly, modified gravity approaches have been successful in explaining the general shape of the observed rotation curves of many dwarf and low surface brightness galaxies, e.g., Swaters et al. (2010), and many other astronomical systems have been interpreted in this context, such as globular clusters (GCs), e.g., Sollima & Nipoti (2010); Haghi et al. (2011); Hernandez & Jiménez (2012), the relative velocity of wide binaries in the solar neighbourhood, e.g., Hernandez et al. (2012), the infall velocity of the two component of the Bullet cluster, e.g., Moffat & Toth (2010) and gravitational lensing of elliptical galaxies, e.g., Mendoza et al. (2012).

One generic prediction of modified gravity theories designed not to require the hypothesis of dark matter, is that

whenever accelerations fall below $a_0 \approx 1.2 \times 10^{-10} \text{ m/s}^2$, a transition should occur away from Newtonian gravity e.g. MOND in Milgrom (1983), TeVeS in Bekenstein (2004), QUMOND, BIMOND in Zhao & Famaey (2010), the extended Newtonian force law in Mendoza et al. (2011) or its relativistic version in Bernal et al. (2011). Regardless of the details, the modified regime will be characterized by equilibrium velocities for test particles orbiting within spherical mass distributions which become constant with distance, and which scale with mass as $V^4 \propto M$.

To test the predictions of modified gravity schemes in elliptical galaxies one needs to know the kinematics and mass distribution of these systems. Elliptical galaxies are hot systems with little or no cold gas where determining their kinematic is more difficult than for spiral galaxies. Their orbital structure is thought to be the result of their evolution through a complex formation process. For determining their dynamics several tracers have been used, such as X-ray gas, GCs and planetary nebulae (PNe). Massive elliptical galaxies are usually surrounded by hot and low density gas evident through its X-ray glow. A tool to determine the mass distribution in these systems is to model their X-ray spectra to obtain density and temperature profiles for the gas, if we assume hydrostatic equilibrium for this component, we can then obtain the mass distribution and then an estimate of the brightness profile to be compared to the photometrically observed one, e.g., Das et al. (2010).

The problem of modeling the luminosity profile and kinematics of elliptical galaxies has been treated before, e.g., Kormendy et al. (2009) modelled the brightness profiles of all known elliptical galaxies in the Virgo cluster using Sersic profiles $\log I \propto r^{1/n}$, they develop a mechanism to calculate a realistic error in the Sersic parameters and identify departures from these profiles that are diagnostic of galaxy formation processes. Teodorescu et al. (2011) studied the kinematics of PNe in the Virgo giant elliptical galaxy NGC 4649 (M 60), assuming Newtonian gravity, they conclude that the kinematics of this object are consistent with the presence of a dark matter halo around M60, this halo is almost one-half of the total mass of the galaxy within $3R_e$. In De Bruyne et al. (2001) three-integral axisymmetric models for NGC 4649 and NGC 7097 are considered, concluding that the kinematic data of NGC 4649 are consistent with a dynamical model with a moderate amount of dark matter, Das et al. (2010) create a dynamical model of NGC 4649 using the NMAGIC code and kinematic constraints to infer a dark matter mass fraction in NGC 4649 of ~ 0.78 at $4R_e$. In Samurović & Čirković (2008a) and Samurović & Čirković (2008b) the GC dynamics of NGC 4649 are used as mass tracers and the Jeans equation is solved for Newtonian and MOND models, finding that both are consistent with the values of the observed velocity profile of the galaxy, although considering the light distribution only to first approximation, as a radial power law for the surface brightness profile.

Following this ideas, in this paper we construct fully self-consistent dynamical models for the massive elliptical galaxy NGC 4649 using the modified Newtonian force law formulation of Mendoza et al. (2011), to explore the consistency of that approach. The free parameters of the galactic model are calibrated to match the details of the observed surface brightness and projected velocity dispersion profiles.

We find that fully self-consistent equilibrium models can be constructed to match all observational constraints available on NGC 4649, including the outward flattening of the projected velocity dispersion profiles, without invoking any dark matter. To within uncertainties, the same happens under Newtonian gravity, but requiring substantial amounts of the hypothetical and as yet undetected dark matter.

In section (2) we derive the model through which equilibrium profiles for spherically symmetric stellar populations are derived, under the modified Newtonian force law of Mendoza et al. (2011). In section (3) we show that such models can be easily obtained to satisfy all observed parameters for NGC 4649, all showing clearly a flattening of their projected velocity dispersion profiles at large radius. Our conclusions appear in section (5).

2 NON-ISOTHERMAL GRAVITATIONAL EQUILIBRIUM MODELS

In the same way as done for globular clusters e.g. Sollima & Nipoti (2010), in Hernandez & Jiménez (2012) we have modeled the massive elliptical galaxy NGC 4649 as a population of self gravitating stars in a spherically symmetric equilibrium configuration, under a modified Newtonian gravitational force law. For a test particle at a distance r from the centre of a spherically symmetric mass distributions $M(r)$:

$$f(x) = a_0 x \left(\frac{1 - x^n}{1 - x^{n-1}} \right). \quad (1)$$

In the above $x = l_M/r$, where $l_M = (GM(r)/a_0)^{1/2}$. We see that when $a \gg a_0$, $x \gg 1$ and $f(x) \rightarrow a_0 x^2$, one recovers Newton's force law, while when $a \ll a_0$, $x \ll 1$ and $f(x) \rightarrow a_0 x$, where an equivalent MOND force law $f = (M(r)G a_0)^{1/2}/r$ is obtained. The index $n > 1$ mediates the abruptness of the transition between the two regimes.

This was shown in Mendoza et al. (2011) to yield generalised isothermal gravitational equilibrium configurations with characteristic finite radii, masses and velocity dispersion values, r_g , M , σ , which smoothly evolve from the classical virial equilibrium of $M = \sigma^2 r_g / G$ to the observed tilt in the fundamental plane of elliptical galaxies, to the $\sigma^4 = (M G a_0)$ scaling of the galactic Tully-Fisher relation, as one goes from $x \gg 1$ to $x \sim 1$ to $x \ll 1$. Also, consistency with solar system observations was found there to constrain the transition to be fairly abrupt, requiring $n > 4$, and in Mendoza et al. (2011) it is also proven that a sufficient condition for Newton's theorems for spherically symmetric mass distributions to hold, for any modified force law, is only that f can be written as a function exclusively of the variable x .

Recently, in Hernandez & Jiménez (2012) we showed that constructing similar successful models for globular clusters requires $n > 10$ to obtain best fits to brightness and velocity dispersion profiles, here we use $n = 10$ to construct equilibrium models for the elliptical galaxy NGC 4649. Notice also that given the form of the proposed force law, any other larger value of n results in only marginal differences from $n = 10$. In addition, Bernal et al. (2011) showed this modified force law model to be the low velocity limit of a formal generalization to GR of the $f(R)$ type, providing a theoretical basis for the model used.

Taking the derivative of the kinematic pressure, the equation of hydrostatic equilibrium for a polytropic equation of state $P = K\rho^\gamma$ is:

$$\frac{d(K\rho^\gamma)}{dr} = -\rho\nabla\phi. \quad (2)$$

In going to locally isotropic Maxwellian conditions, $\gamma = 1$ and $K = \sigma(r)^2$ and we get:

$$2\sigma(r)\frac{d\sigma(r)}{dr} + \frac{\sigma^2(r)}{\rho}\frac{d\rho}{dr} = -\nabla\phi. \quad (3)$$

since $\rho = (4\pi r^2)^{-1} \frac{dM(r)}{dr}$ the preceding equation can be written as:

$$\begin{aligned} 2\sigma(r)\frac{d\sigma(r)}{dr} + \sigma(r)^2 \left[\left(\frac{dM(r)}{dr} \right)^{-1} \frac{d^2 M(r)}{dr^2} - \frac{2}{r} \right] \\ = -a_0 x \left(\frac{1-x^n}{1-x^{n-1}} \right), \end{aligned} \quad (4)$$

where $\sigma(r)$ is the isotropic Maxwellian velocity dispersion for the population of stars, which is allowed to vary with radius, as observed in NGC 4649, e.g., Pinkney et al. (2003). The above is a generalization of the treatment presented in Hernandez et al. (2010), which we used in the modeling of dSph galaxies, which are characterized by flat velocity dispersion profiles, obtaining mass models consistent with observed velocity dispersion, half mass radii and total masses, in the absence of dark matter. Another example of a similar treatment is found in Hernandez & Jiménez (2012), where we modeled eight GCs in our Galaxy proposing a function $\sigma(r)$ for modeling the velocity dispersion profile of GCs assuming the same modified law of gravity used here, accurately reproducing all observational constraints.

As an illustrative example we can take the limit $f(x) = a_0 x^2$, and recover $-GM(r)/r^2$ for the right hand side of equation (3), the Newtonian expression appearing for $a \gg a_0$, or equivalently $x \ll l_M$. If one then imposes isothermal conditions $\sigma(r) \equiv \sigma$ and looks for a power law solution for $M(r) = M_0(r/r_0)^m$, we get:

$$\sigma^2 \left[\frac{m-3}{r} \right] = -\frac{GM_0}{r^2} \left(\frac{r}{r_0} \right)^m, \quad (5)$$

and hence $m = 1$, the standard isothermal halo, $M(r) = 2\sigma^2 r/G$, having a constant centrifugal equilibrium velocity $v^2 = 2\sigma^2$ and infinite extent. At the other limit, $a \ll a_0$, $x \gg l_M$, equation (3) yields:

$$\sigma^2 \left[\frac{m-3}{r} \right] = -\frac{[GM_0 a_0]^{1/2}}{r} \left(\frac{r}{r_0} \right)^{m/2}. \quad (6)$$

In this limit $m = 0$, we obtain $M(r) = M_0$ and $v^2 = 3\sigma^2 = (GM_0 a_0)^{1/2}$, the expected Tully-Fisher scaling of the circular equilibrium velocity with the fourth root of the mass, with rotation velocities which remain flat even after the mass distribution has converged, rigorously isothermal halos are naturally limited in extent. It is interesting to note that in this limit the scaling between the circular rotation velocity and the velocity dispersion is only slightly modified as compared to the Newtonian case, the proportionality constant changes from 2 to 3, for the squares of the velocities. In astrophysical units, this low acceleration limit for an isothermal halo in gravitational equilibrium yields:

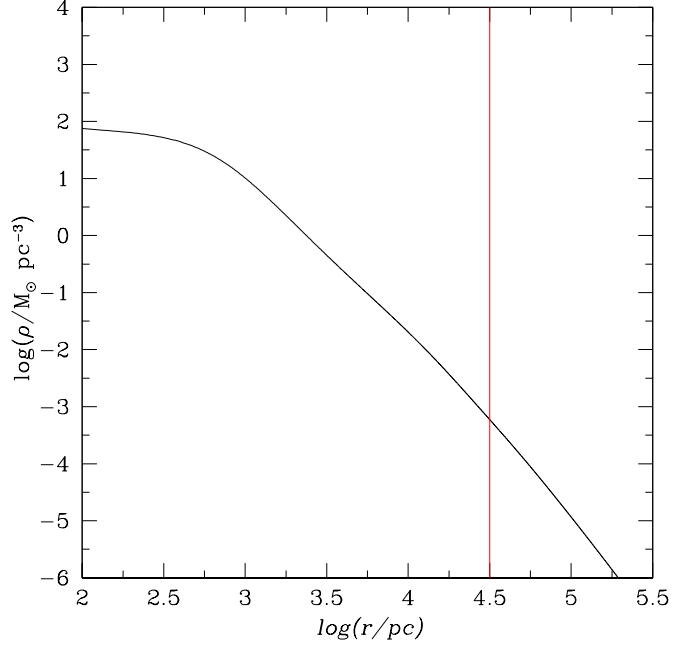


Figure 1. Volumetric density profile for the best fit model for NGC 4649. The vertical line gives the point where $x = 1$. Note that the asymptotic $\rho(r)$ profile at large radii is steeper than the r^{-2} of the Newtonian case, resulting in a finite total radius and total mass for the configuration.

$$\sigma = 0.2 \left(\frac{M_0}{M_\odot} \right)^{1/4} \text{ km/s}, \quad (7)$$

$$v = 0.35 \left(\frac{M_0}{M_\odot} \right)^{1/4} \text{ km/s}, \quad (8)$$

for the velocity dispersion and the centrifugal equilibrium velocities of a halo of total mass M_0 , respectively.

Taking initial conditions $M(r) \rightarrow 0$, $dM(r)/dr \rightarrow 4\pi r^2 \rho_0$, when $r \rightarrow 0$, a constant central density ρ_0 , we can solve the full second-order differential equation (4) for $M(r)$ through a numerical finite differences scheme, once a model for $\sigma(r)$ is adopted.

Solving equation (4) yields the volumetric profiles for the density and mass, $\rho(r)$, $M(r)$. $\rho(r)$ is then projected along one dimension to obtain a projected surface density mass profile, $\Sigma(R)$. In all that follows we shall use r for radial distances in 3D, and R for a projected radial coordinate on the plane of the sky. $\Sigma(R)$ can be compared to observed surface brightness profiles once a mass-to-light ratio is assumed.

Finally, a projected velocity dispersion profile $\sigma_p(R)$ is constructed through a volume density weighted projection of the volumetric velocity dispersion profile of a model, $\sigma(r)$. Therefore, a proposed model for $\sigma(r)$ does not directly give a projected $\sigma_p(R)$ profile, which the model only yields after having solved for the detailed density structure, and the subsequent mass weighted projection of the proposed $\sigma(r)$.

Observations provide only the density weighted projected profiles of $\sigma(r)$, integrated along the line of sight, $\sigma_p(R)$, not the volumetric $\sigma(r)$ profiles which we require in equation (4). We shall therefore adopt a parametric form

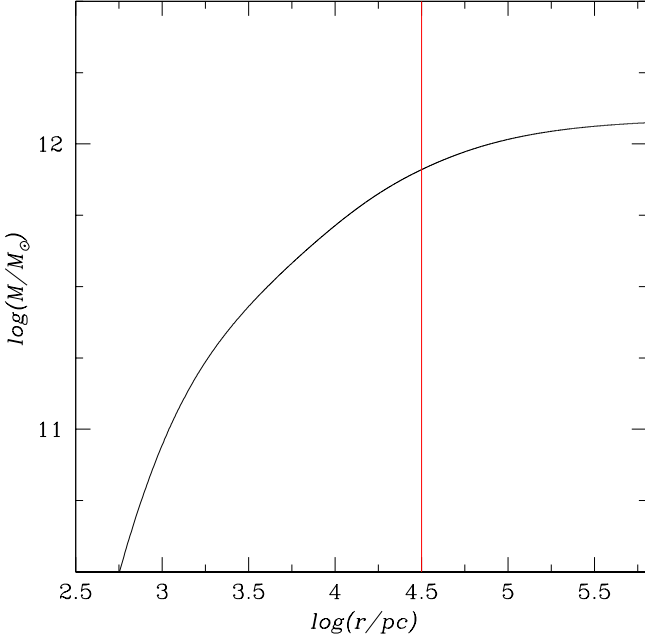


Figure 2. Volumetric mass profile for the best fit model for NGC 4649. The vertical line gives the point where $x = 1$. Note that the total mass converges for a finite radius.

for the volumetric velocity dispersion profile, and adjust the parameters to obtain a match to the observed galactic properties. For this we use:

$$\sigma(r) = \sigma_1 \exp\left(-\frac{r}{r_\sigma}\right) + \sigma_\infty. \quad (9)$$

In the above σ_∞ is given directly by the observations as the asymptotic value of the measured projected velocity dispersion profile for the galaxy, this value is $\approx 200 \text{ km s}^{-1}$, Das et al. (2011), as at larger R radii, projection effects tend to zero and $\sigma(R) \rightarrow \sigma(r)$. This leaves us with three model parameters to determine: ρ_0 , σ_1 and r_σ , which we fit to match the observed projected velocity dispersion profile, as well as a central projected velocity dispersion value for NGC 4649 of $\approx 400 \text{ km s}^{-1}$ Pinkney et al. (2003), and comparing the resulting model $\Sigma(R)$ profile to the observed surface brightness profile of NGC 4649, taking $M/L = 8.0$, following Bridges et al. (2006).

3 MODELLING ELLIPTICAL GALAXY NGC 4649

We begin this section presenting in figures (1) and (2) our best fit NGC 4649 model. In figure (1) we show the volumetric density profile, which is qualitatively similar to a cored isothermal profile, with the difference that the asymptotic $\rho(r)$ profile at large radii is steeper than the r^{-2} of the Newtonian case. This results in finite total masses and finite half-mass radii even for the asymptotically flat $\sigma(r)$ volumetric profiles we adopt, in contrast with the situation in classical gravity, where infinitely extended mass profiles would appear. This finite profiles are also what appears under the type of modified gravity laws we are treating, even for rig-

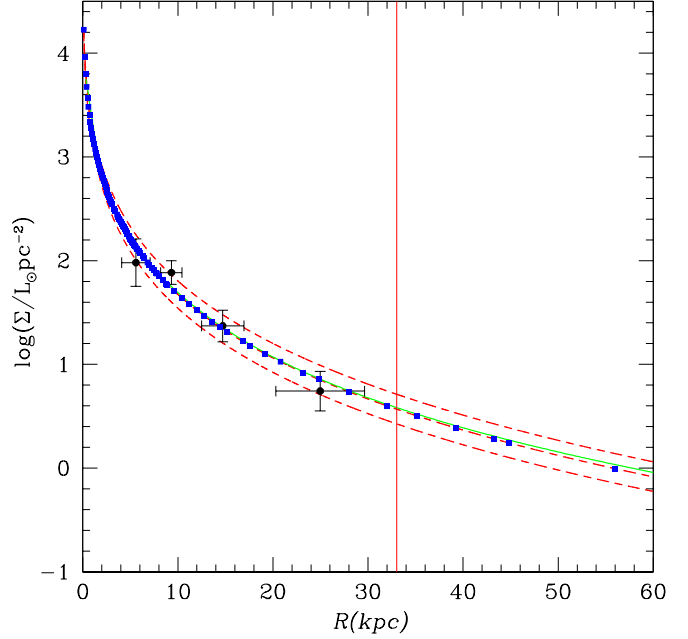


Figure 3. Comparison of the resulting model projected surface brightness for NGC 4649 (thick continuous line) to the corresponding observed quantities and the best fit Sersic function with the central (dashed line), maximum and minimum values consistent with the reported confidence intervals for the Sersic parameters, flanking curves. The squares correspond to data in (Kormendy et al. 2009), and the points with error bars for PNe data, (Teodorescu et al. 2011) Following Bridges et al. (2006) we take $M/L_V = 8$, which coincides with the stellar population studies on Shen & Gebhardt (2010). The vertical line gives the point where $x = 1$ and the modified force law used shifts from the classical Newtonian form to the MONDian character of eq.(6)

orously isothermal $\sigma(r) = \sigma_0$ equilibrium configurations, as already pointed out in Hernandez et al. (2010) and Mendoza et al. (2011) and as shown in the developments following eq. (6). The vertical line shows the radius where the condition $x = 1$ is crossed, i.e., the point beyond which $a < a_0$, and hence the departure of the force law used from the Newtonian value towards the MONDian regime, consequently the point where the density profile steepens away from the $1/r^2$ of Newtonian gravity, towards the convergence of the MONDian regime.

Figure (2) shows the corresponding volumetric radial mass profile for the same model, indicating again with a vertical line the threshold where $x = 1$. This clearly shows the departure from the linear growth of the total mass within the approximately isothermal Newtonian region, towards convergence to a finite total mass in the MONDian $a < a_0$ regime. We see that 40% of the total model mass lies beyond $x = 1$. This fraction is distributed over a much larger area having much smaller projected mass surface densities than the central regions interior to the $x = 1$ threshold, the ones which are much more easily observed, and over which Newtonian gravity accurately holds.

These two figures illustrate the physical consistency of the model, a positive isotropic Maxwellian volumetric velocity dispersion is assumed, integration of eq.(4) then yields

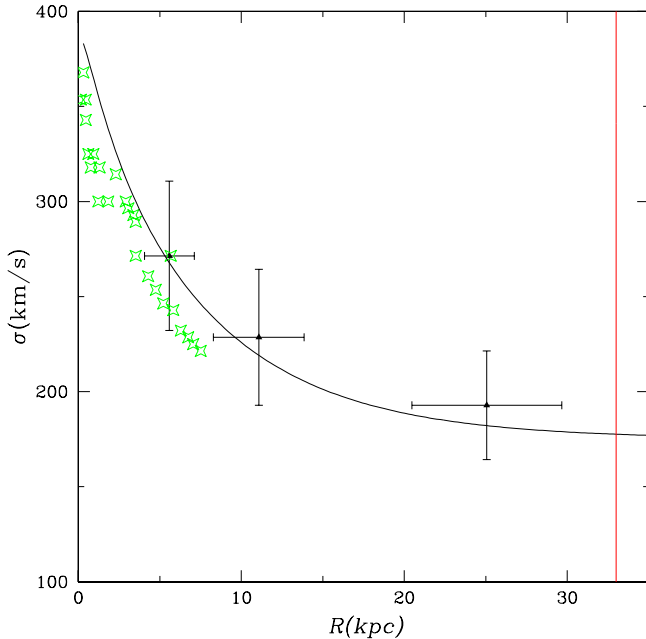


Figure 4. Comparison of the resulting model projected velocity dispersion profile for NGC 4649 (continuous line) to the corresponding observed quantities, stars for long slit observations in (Pinkney et al. 2003) and the points with error bars for PNe data. The vertical line gives the point where $a = a_0$.

a volumetric density profile essentially consistent with what would appear under Newtonian dynamics in the region interior to $x = 1$, where the force law converges precisely to the standard expression. At large radii however, the density profile increasingly steepens and naturally reaches $\rho(r) = 0$ at a well defined total radius, as is evident from the convergence seen in figure (2). Thus, the distribution function is necessarily positive throughout the modeled structure, and goes to zero at a well defined outer radius.

The best fit model constructed as described above was optimised to match the inferred total mass, the observed projected surface brightness profile under the assumption of constant M/L_V , and the projected velocity dispersion measurements. We take the surface brightness profile observations from photometry in Kormendy et al. (2009) and the scaled number density calculated from PNe in Teodorescu et al. (2011) as presented in Das et al. (2011), and projected velocity dispersion measurements from Pinkney et al. (2003) adapted in De Bruyne et al. (2001). Following Bridges et al. (2006) we take $M/L_V = 8$, which coincides with the central value reported by Shen & Gebhardt (2010) determined directly from stellar population synthesis models.

The final resulting surface brightness profile and its corresponding volume density weighted projected velocity dispersion profile $\sigma_p(R)$ for galaxy NGC 4649 are presented in figures 3 and 4, the parameters for the best fit in eq.(9) are $\sigma_\infty = 175 \text{ km/s}$, $\sigma_1 = 230 \text{ km/s}$ and $r_\sigma = 8.5 \text{ kpc}$, the central density that we have assumed is $\rho_0 = 1.5 \times 10^2 M_\odot/\text{pc}^3$. In the figures the vertical line indicates the point where $a = a_0$, we can see that the model accurately fits the observed projected surface brightness profiles of the galaxy and the central value of the measured projected velocity disper-

sion $\sigma_p(R = 0) = 400 \text{ km/s}$, as well as the observed profiles for $\sigma_p(R)$.

We see that both, the surface brightness and velocity dispersion profiles are in agreement with photometry and PNe observations, to within reported uncertainties. Under Newtonian gravity this requires to invoke a large amount of dark matter to reproduce the structure and kinematics of this galaxy, while under the modified force law scheme treated here, it is a natural consequence of the change in gravitational regime, leading to finite matter distributions when $a < a_0$ and $\sigma(r)$ tends to a constant.

The total mass we obtain from the dynamical modeling described is consistent with what results from the integration of the surface brightness profile assuming a constant mass to light ratio $M/L_V = 8$. The mass obtained for the dynamical model to NGC 4649 is $1.09 \times 10^{12} M_\odot$, and the luminosity that results from integrating the V band light profile is $1.36 \times 10^{11} L_\odot$, implying a mass of $1.08 \times 10^{12} M_\odot$ from using $M/L_V = 8$ as determined directly from the stellar population studies of Shen & Gebhardt (2010). Also, notice that the asymptotic value of the velocity dispersion is $195.0 \pm 30.36 \text{ km/s}$ in consistency with the $\sigma = 0.2(M/M_\odot)^{1/4} = 203.9 \text{ km/s}$ prediction of eq. (7) for $1.08 \times 10^{12} M_\odot$.

4 CONCLUSIONS

We show that for the massive elliptical galaxy NGC 4649, fully self consistent spherically symmetric equilibrium models can be constructed using a modified Newtonian force law which smoothly transits from the Newtonian value when $a > a_0$, towards the MONDian phenomenology in the $a < a_0$ regime, which naturally satisfy all observational constraints available for the central, asymptotic and radial profiles for projected surface brightness and velocity dispersion measurements. All this, without the need of invoking any hypothetical and as yet undetected dark matter component.

The resulting models are typically characterized by a Newtonian inner region, which smoothly transits to a modified gravity outer region on crossing the $a = a_0$ threshold. The resulting internal velocity dispersion profiles correspondingly transit from an inner radially decaying region to an outer flat velocity dispersion one.

We show that the asymptotic value of the measured velocity dispersion profile, $\sigma_p(R \rightarrow \infty)$, and the total mass for this systems, M , are consistent with the generic modified gravity prediction for $\sigma_p(R \rightarrow \infty) = 0.2(M/M_\odot)^{1/4}$.

ACKNOWLEDGEMENTS

Xavier Hernandez acknowledges financial assistance from UNAM DGAPA grant IN103011-3. Alejandra Jimenez acknowledges financial support from a CONACYT scholarship.

REFERENCES

- Bekenstein J. D., 2004, Phys. Rev. D, 70, 083509
- Bernal T., Capozziello S., Hidalgo J. C., Mendoza S., 2011, Eur. Phys. J. C, 71, 1794

- Bosma A., 1981, *AJ*, 86, 1825
- Bridges T., Gebhardt K., Sharples R., Faifer F. R., Forte J. C., Beasley M. A., Zepf S. E., Forbes D. A., Hanes D. A., Pierce M., 2006, *MNRAS*, 373, 157
- Das P., Gerhard O., Churazov E., Zhuravleva I., 2010, *MNRAS*, 409, 1362
- Das P., Gerhard O., Mendez R. H., Teodorescu A. M., de Lorenzi F., 2011, *MNRAS*, 415, 1244
- De Bruyne V., Dejonghe H., Pizzella A., Bernardi M., Zeilinger W. W., 2001, *ApJ*, 546, 903
- Haghi H., Baumgardt H., Kroupa P., 2011, *A&A*, 527, A33
- Hernandez X., Jiménez M. A., 2012, *ApJ*, 750, 9
- Hernandez X., Jiménez M. A., Allen C., 2012, *European Physical Journal C*, 72, 1884
- Hernandez X., Mendoza S., Suarez T., Bernal T., 2010, *A&A*, 514, A101
- Kormendy J., Fisher D. B., Cornell M. E., Bender R., 2009, *ApJS*, 182, 216
- Kroupa P., Famaey B., de Boer K. S., Dabringhausen J., Pawlowski M. S., Boily C. M., Jerjen H., Forbes D., Hensler G., Metz M., 2010, *A&A*, 523, A32
- McGaugh S. S., de Blok W. J. G., 1998, *ApJ*, 499, 41
- McGaugh S. S., Wolf J., 2010, *arXiv:1003.3448*
- Mendoza S., Bernal T., Hernandez X., Hidalgo J. C., Torres L. A., 2012, *ArXiv e-prints*
- Mendoza S., Hernandez X., Hidalgo J. C., Bernal T., 2011, *MNRAS*, 411, 226
- Milgrom M., 1983, *ApJ*, 270, 365
- Moffat J. W., Toth V. T., 2010, *ArXiv e-prints*
- Pinkney J., Gebhardt K., Bender R., Bower G., Dressler A., Faber S. M., Filippenko A. V., Green R., Ho L. C., Kormendy J., Lauer T. R., Magorrian J., Richstone D., Tremaine S., 2003, *ApJ*, 596, 903
- Romanowsky A. J., Douglas N. G., Arnaboldi M., Kuijken K., Merrifield M. R., Napolitano N. R., Capaccioli M., Freeman K. C., 2003, *Science*, 301, 1696
- Rubin V. C., Ford Jr. W. K., Thonnard N., Burstein D., 1982, *ApJ*, 261, 439
- Samurović S., Ćirković M. M., 2008a, *A&A*, 488, 873
- Samurović S., Ćirković M. M., 2008b, *Serbian Astronomical Journal*, 177, 1
- Sanders R. H., McGaugh S. S., 2002, *ARA&A*, 40, 263
- Shen J., Gebhardt K., 2010, *ApJ*, 711, 484
- Simon J. D., Geha M., 2007, *ApJ*, 670, 313
- Sollima A., Nipoti C., 2010, *MNRAS*, 401, 131
- Swaters R. A., Sanders R. H., McGaugh S. S., 2010, *ApJ*, 718, 380
- Teodorescu A. M., Méndez R. H., Bernardi F., Thomas J., Das P., Gerhard O., 2011, *ApJ*, 736, 65
- Zhao H., Famaey B., 2010, *Phys. Rev. D*, 81, 087304